by high temperature rather than simply a low Si abundance in the LMC.

11. Estimation of L and n_c, the luminosity and number of ionizing photons, is complicated by two major uncertainties: contamination of the spectrum of R136a by other stars and the large and peculiar extinction by dust. If all the visual light of R136 arises from R136a, with T = 50,000 K, apparent visual magnitude V = 10 (3), distance d = 55 kpc, and visual extinction A_V = 1.8 magnitudes, then $L \approx 7 \times 10^7\ L_\odot$ and $n_c \approx 4 \times 10^{51}$ sec^{-1}. Photographs (3) suggest that R136a is responsible for most but not all of the visual radiation from R136. Hence $L \approx 5 \times 10^7\ L_\odot$ and $n_c \approx 3 \times 10^{51}$ sec^{-1} are not unreasonable estimates. If the temperature of R136a is 60,000 K, L and n_c would approximately double under the same assumptions. It is difficult to estimate A_V. We used various nebular Balmer line/radio continuum ratios to estimate the extinctions at Hα and Hβ [for example, see (2)]. By interpolation, we obtained A_V between 1.6 and 2.1 mag. We consider it reasonable to assign the same extinction to R136a. While some of the nebular dust may be behind the star, thus not contributing to the stellar extinction, the nebular Balmer lines are affected primarily by the absorption of the dust (as opposed to scattering). For the Balmer lines, the absorption of Galactic dust is less than half the extinction [B. D. Savage and J. S. Mathis, *Annu. Rev. Astron. Astrophys.* **17**, 73 (1979), sect. 3.1], so our assumed extinction is probably conservative. The colors of R136 suggest a color excess of $E(B - V)$ = 0.38 [F. P. Israel and J. Koornneef, *Astrophys. J.* **230**, 390 (1979)]. Using $A_V/E(B - V)$ = 4.65 derived from the Balmer lines, we find A_V = 1.8. However, the dust near R136 is likely to be peculiar; for instance, the UV extinction of R136 (6) is somewhat different from that of the general LMC. The extinction for the UV is even more difficult to estimate than for the visual. We suggest that it is about A(1400 Å) = 4 ± 1 mag, based on A(3000 Å) − A_V = 1.5 as derived from the Galactic and LMC extinction laws, A_V = 1.8 mag, and A(1400 Å) − A(3000 Å) = 1.3 mag from IUE observations (6). If we assume that A(1400 Å) = 4 mag and that R136a is responsible for 70 percent of the large-aperture 1400 Å flux, we find $L \approx 5 \times 10^7\ L_\odot$ and $n_c \approx 3 \times 10^{51}$ sec^{-1} for 50,000 K, and values ~ 1.5 times larger for 60,000 K.
12. P. S. Conti and C. D. Garmany, *Astrophys. J.* **238**, 190 (1980); R. P. Kudritzski, *Astron. Astrophys.* **85**, 174 (1980).
13. High-dispersion IUE observations of HD 5980 (OB?+WN3) in the Small Magellanic Cloud obtained by one of us (B.D.S.) reveal P Cygni lines of N V, C IV, He II, and N IV. The stellar Si IV is very weak, as in R136a. A photospheric O V 1371 Å feature is present. The absorption part of the C IV profile saturates. The edge of this line implies a terminal speed of 2800 km sec^{-1}.
14. We recently learned that G. Weigelt (private communication) has speckle interferometry measurements of R136a with the ESO 3.6-m telescope at La Silla, Chile. He has not completed the reduction of his data, but his preliminary results indicate that R136a consists of two objects with a magnitude difference of 2 in a complicated background. This seems in accord with our conclusion that a single object dominates the UV spectrum. We thank Dr. Weigelt for permission to cite his results before publication.
15. D. C. Abbott, J. H. Bieging, E. B. Churchwell, J. P. Cassinelli, *Astrophys. J.* **238**, 196 (1980).
16. Estimated from the models of J. P. Cassinelli and G. L. Olson, *ibid.* **229**, 304 (1979).
17. G. W. Wares and L. H. Aller, *Publ. Astron. Soc. Pac.* **80**, 568 (1968).
18. D. P. Cox and W. H. Tucker [*Astrophys. J.* **157**, 1157 (1969)] showed that collisional ionization of He$^+$ is negligible even if the temperatures of the wind are 60,000 to 70,000 K.
19. D. Hummer and D. Mihalas [*Jt. Inst. Lab. Astrophys. Rep. 101* (1970)], D. Mihalas [*Natl. Ctr. Atmos. Res. Tech. Note NCAR-TN STR-76* (1972)], and R. L. Kurucz [*Astrophys. J. Suppl.* **40**, 1 (1979)] are in good agreement about the gross properties of the spectrum of hot stars. Hummer and Mihalas tabulated the H and He$^+$ ionizing fluxes that were used in Table 2.
20. D. C. Abbott, *Astrophys. J.* **225**, 893 (1978).
21. The electron scattering fails for a cluster of stars because one needs the entire volume of the cluster optically thick in electrons, which requires huge mass loss rates from the cluster—several $M_\odot$ per year. We can reject two-photon emission from H filling in the C IV profile, because such a cloud of ionized gas would produce far too much Balmer line radiation. High densities only make the situation worse because two-photon emission is quenched first.
22. F. Hoyle and W. A. Fowler, *Mon. Not. R. Astron. Soc.* **125**, 169 (1963). For a lengthy discussion of polytropes, see S. Chandrasekhar, *An Introduction to the Study of Stellar Structure* (Univ. of Chicago Press, Chicago, 1930).
23. M. Schwarzschild and R. Harm, *Astrophys. J.* **129**, 637 (1959); K. Ziebarth, *ibid.* **162**, 947 (1970); C. de Jager, *The Brightest Stars* (Reidel, Dordrecht, Netherlands, 1980).
24. H. Yorke, *Int. Astron. Union Symp. 42* (1978), p. 38.
25. S. Kwok, *Astrophys. J.* **198**, 583 (1975); J. P. Cassinelli, *Annu. Rev. Astron. Astrophys.* **17**, 275 (1979).
26. We expect on the basis of x-ray observations of O and B supergiants (J. P. Cassinelli *et al.*, *Astrophys J.*, in press) that the x-ray luminosity of the star might be of order $10^{-7.5}\ L_{bol}$ (10^{34} erg sec^{-1}), where L_{bol} is the bolometric luminosity, and some of this would be attenuated by intervening interstellar matter [hydrogen column density = 7×10^{21} (9)]. A dense cluster of O stars, on the other hand, might be a strong x-ray source because of the collision of the various stellar winds [B. A. Cooke, A. C. Fabian, J. E. Pringle, *Nature (London)* **273**, 645 (1978)]. A shock at the interface of the observed outflow and the surrounding interstellar medium might also be a source of hard x-rays [J. Castor, R. McCray, R. Weaver, *Astrophys. J. Lett.* **200**, L107 (1975)].
27. IUE low-dispersion spectra of supergiant H II regions have been published: NGC 604 in M33 and NGC 5471 in M101 by M. Rosa [*Astron. Astrophys.* **85**, L21 (1980)] and regions in NGC 2366 and K 2574 by P. M. Gondhalekhar, D. H. Morgan, K. Nandy, and R. Wilson [in *Second European IUE Conference* (ESA-Sp-157, European Space Agency, Paris, 1980), p. 131]. The spectrum of NGC 604 appears to be compatible with that of a cluster of normal O stars (strong Si IV); NGC 5471 has a spectrum resembling that of an exceedingly hot object.
28. B.D.S. is a guest observer with the IUE satellite, which is sponsored and operated by the National Aeronautics and Space Administration, the Science Research Council of the United Kingdom, and the European Space Agency. We thank the entire IUE staff at Goddard Space Flight Center for their assistance in acquiring and processing the IUE data included in this report. We thank M. R. Meade for her assistance with the data processing. B.D.S. acknowledges support from NASA grants NSG 5241 and 5363, J.P.C. from NSF grant AST-7912141, and J.S.M. from NSF grant AST-7906829. Useful comments on the manuscript were provided by a number of colleagues, especially L. Hartmann.

12 February 1981; revised 29 April 1981

Solar Flare Acceleration of Solar Wind: Influence of Active Region Magnetic Field

Abstract. *The direction of the photospheric magnetic field at the site of a solar flare is a good predictor of whether the flare will accelerate solar wind plasma. If the field has a southward component, high-speed solar wind plasma is usually observed near the earth about 4 days later. If the field has a northward component, such high-speed solar wind is almost never observed. Southward-field flares may then be expected to have much larger terrestrial effects than northward flares.*

Solar flares that occur in active regions where the photospheric magnetic field has a southward component tend to be associated with enhanced solar wind velocity observed near the earth 4 days later. This was observed in both the northern and southern solar hemispheres during portions of the last two 11-year sunspot cycles. During most of the time interval investigated, the solar field polarity was outward in the north and inward in the south.

For this report we used all the flares in the interval 24 August 1978 through 9 November 1979 with importance 2 or greater, as reported by the group observations in Solar-Geophysical Data (*1*). Flares whose disk longitude exceeded 70° were not used. The start of the interval was determined by the beginning of observations by the Los Alamos solar wind experiment on the spacecraft International Sun-Earth Explorer 3 (ISEE-3), and the end of the interval was selected

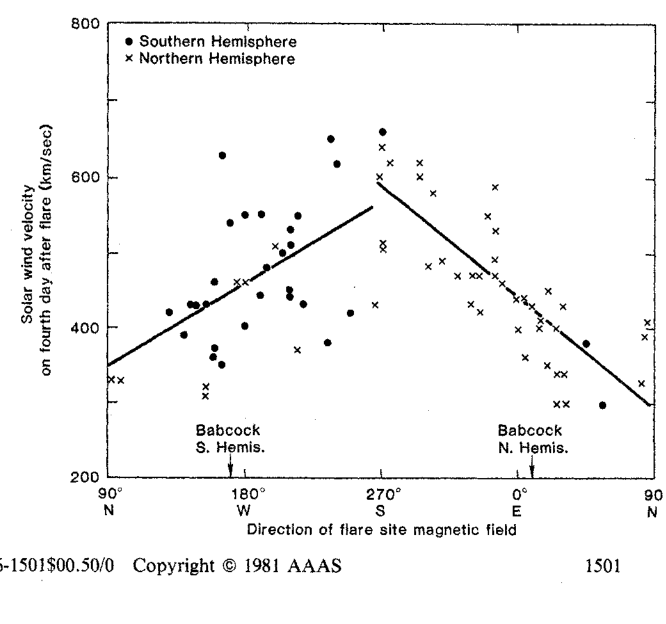

Fig. 1. Solar wind velocity observed near the earth on the fourth day after a flare as a function of the direction of the flare-site photospheric magnetic field.

to be well before the change in polarity of the solar polar magnetic fields. A list of the 80 flares used in this study is available from the authors. We obtained very similar results for the interval May 1967 to August 1972 and the interval June 1977 to August 1978; thus the effect is long lasting and significant.

At the site of each flare the direction of the photospheric magnetic field was measured by using the Mount Wilson and Kitt Peak observations reported in Solar-Geophysical Data (*1*). A transparent straight edge was used to determine the approximate direction of the line dividing the two polarities of the magnetic field at the site of the flare, and the field direction was taken to be perpendicular to this line.

Figure 1 shows the average solar wind velocity on the fourth day after the flare (that is, averaged over 72 to 96 hours after the flare) as a function of the direction of the photospheric magnetic field at the site of the flare. A tendency can be seen for the southward flares to be associated with higher solar wind velocity and the northward flares with lower velocity, with a smooth progression between the extremes. The two solid lines are separate least-squares fits to the data.

Flares in the northern solar hemisphere are represented in Fig. 1 with crosses, and those in the southern hemisphere with dots. The arrows indicate the field direction in each hemisphere given by the model of Babcock (*2*). Most of the northern hemisphere flares are clustered about the direction indicated for the Babcock model in the northern hemisphere, and the same is true for the southern hemisphere.

Figure 2 shows a superposed epoch analysis of the average solar wind velocity observed in the interval from 10 days before the time of the flare to 10 days after. The solid line represents 39 flares whose sites had a photospheric field, *B*, with a southward component and the dashed curve represents 32 northward flares. Nine flares had fields directed approximately parallel to the solar equator and are not included in Fig. 2. The southward flares are on the average clearly associated with high-speed solar wind, while the northward flares are on the average not associated with increased solar wind velocity.

We discovered the effect described here while investigating the influence of the direction of the flare-site magnetic field on geomagnetic activity reported by Pudovkin and co-workers (*3*). They reported that southward (defined by them with respect to the geomagnetic field

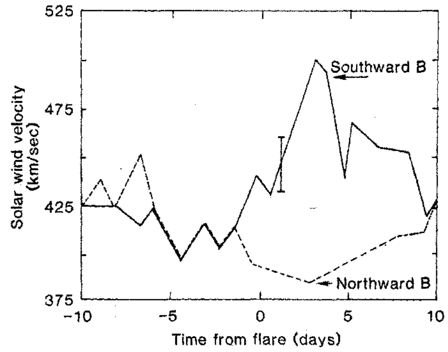

Fig. 2. Superposed epoch plot of average solar wind velocity observed near the earth. Zero time is the time of the flare. The error bar represents twice a typical standard error of the mean. This is not a direct test of significance since a single active region sometimes produced more than one flare, and flares sometimes occurred within a few days of each other, so that the flare events are not completely independent.

rather than the solar magnetic field) flares produced geomagnetic activity and that northward flares did not. They also reported that southward flares accelerated solar wind plasma having a southward component of interplanetary magnetic field and that northward flares had a northward component of interplanetary magnetic field. The effect reported here may aid in the prediction of terrestrial consequences of solar flares.

H. LUNDSTEDT
J. M. WILCOX
P. H. SCHERRER
Institute for Plasma Research, Stanford University, Stanford, California 94305

References and Notes

1. Solar-Geophysical Data, National Geophysical and Solar-Terrestrial Data Center, Boulder, Colo.
2. H. W. Babcock, *Astrophys. J.* **133**, 572 (1961).
3. M. I. Pudovkin and A. D. Chertkov, *Sol. Phys.* **50**, 213 (1976); M. I. Pudovkin, S. A. Zaitseva, I. P. Oleferenko, A. D. Chertkov, *ibid.* **54**, 155 (1977); M. I. Pudovkin, S. A. Zaitseva, E. E. Benevolenska, *J. Geophys. Res.* **84**, 6649 (1979).
4. We thank the Los Alamos group for the use of their ISEE-3 solar wind plasma observations, and G. Borrini, R. Clauer, P. Duffy, J. Foster, T. Hoeksema, R. Howard, and S. Suess for helpful comments. This work was supported in part by ONR contract N00014-76-C-0207, NASA grant NGR05-020-559 and contract NAS5-24420, NSF grant ATM80-20421, and the Max C. Fleischmann Foundation.

17 February 1981

Eastern Indian 3800-Million-Year-Old Crust and Early Mantle Differentiation

Abstract. *Samarium-neodymium data for nine granitic and tonalite gneisses occurring as remnants within the Singhbhum granite batholith in eastern India define an isochron of age* $3775 \pm 89 \times 10^6$ *years with an initial* $^{143}Nd/^{144}Nd$ *ratio of* 0.50798 ± 0.00007. *This age contrasts with the rubidium-strontium age of* 3200×10^6 *years for the same suite of rocks. On the basis of the new samarium-neodymium data, field data, and petrologic data, a scheme of evolution is proposed for the Archean crust in eastern India. The isotopic data provide evidence that parts of the earth's mantle were already differentiated with respect to the chondritic samarium-neodymium ratio* 3800×10^6 *years ago.*

This report describes the samarium-neodymium systematics, geology, and petrology of a group of granitic rocks from the Singhbhum-Orissa iron ore province in eastern India. The purpose of the study is to obtain a precise samarium-neodymium age for these rocks, to determine the sources and evolution of the ancient granitic crust in this part of India, and to evaluate the nature of differentiation of the Archean mantle.

The oldest known granitic rocks (3.5×10^9 to 3.8×10^9 years) have been reported from western Greenland, Labrador, Minnesota, and Michigan (*1, 2*). Granites and granitic gneisses occupy large areas of the Indian shield, and it has long been suspected that granitic rocks of Archean age (greater than 2.5×10^9 years) occur in India. Although some of the high-grade granitic gneisses in the Indian shield are very similar to the oldest gneisses in Greenland, the available radiometric dating by the potassium-argon and rubidium-strontium methods suggests ages no older than 3.5×10^9 years (*3*). The samarium-neodymium method (*4*) is considered a more reliable way of dating ancient rocks because of the relatively greater stability of samarium and neodymium as compared with other known radioactive parent-daughter pairs (*5*). We report here the first samarium-neodymium study on a group of Indian Archean granites.

The vast Singhbhum granite batholith complex occupies over 10,000 km^2 in the Singhbhum-Orissa iron ore province of the Indian shield (*6*). The oldest unit in this complex is a biotite-tonalite gneiss grading to granodiorite which occurs as numerous remnants within the main mass of Singhbhum granite. The largest of these tonalite-gneiss remnants occu-